

## Alpha-deuteron structure of ${}^6\text{Li}$ as predicted by three-body models

D. R. Lehman

*Department of Physics, The George Washington University, Washington, D.C. 20052*

Mamta Rajan

*Computer Sciences Corporation, Silver Spring, Maryland 20910*

(Received 18 September 1981)

Three-body ( $\alpha NN$ ) models of the  ${}^6\text{Li}$  ground state are used to examine its alpha-deuteron structure. Three models of the  ${}^6\text{Li}$  ground-state wave function are considered: simple, full (0%), and full (4%). The full (4%) model is derived by solving the Schrödinger equation with the  ${}^3S_1$ - ${}^3D_1$   $n$ - $p$  interaction (4%  $D$  state in the deuteron) plus the  $S_{1/2}$ ,  $P_{1/2}$ , and  $P_{3/2}$   $\alpha$ - $N$  interactions, whereas the full (0%) and simple models truncate the  $n$ - $p$  interaction to only the  ${}^3S_1$  component and the simple model also drops the  $S_{1/2}$  and  $P_{1/2}$  components of the  $\alpha$ - $N$  interaction. These models are used to calculate the  $s$ - and  $d$ -wave  ${}^6\text{Li} \rightarrow \alpha + d$  momentum distributions, the percentage of  $s$ - and  $d$ -wave  $\alpha$ - $d$  components in the  ${}^6\text{Li}$  wave functions, the effective  $s$ - and  $d$ -wave configuration-space wave functions, and the  $S$ - and  $D$ -wave  ${}^6\text{Li} \rightarrow \alpha + d$  asymptotic normalization constants. The most sophisticated of the models, full (4%), predicts a  ${}^6\text{Li} \rightarrow \alpha + d$  momentum distribution in agreement at low momentum transfers ( $q \leq 0.3 \text{ fm}^{-1}$ ) with the latest momentum distribution extracted from a 670 MeV  ${}^6\text{Li}(p, pd)\alpha$  experiment; a 65.4%  $\alpha$ - $d$  component in the  ${}^6\text{Li}$  wave function with only 0.049% coming from the  $d$ -wave contribution; that both the  $s$ - and  $d$ -wave effective  $\alpha$ - $d$  wave functions have nodes at  $\sim 1.6$  and  $\sim 1.65$  fm, respectively, though they differ in shape; and the values of the  ${}^6\text{Li} \rightarrow \alpha + d$ ,  $S$ - and  $D$ -wave asymptotic normalization constants to be 2.182 and 0.0178, respectively, consistent with present experimental values. Detailed comparison between the models is made, especially with respect to the role of the  $n$ - $p$  tensor force and repulsive  $S_{1/2}$   $\alpha$ - $N$  interaction. The character of the  $\alpha$ - $d$   $d$ -wave component is thoroughly examined.

[ NUCLEAR STRUCTURE  ${}^6\text{Li}$ , three-body models, asymptotic norms,  
spectroscopic factors, momentum distributions. ]

### I. INTRODUCTION

Evidence is mounting that the low-energy properties and dynamics of the  $A = 6$  system can be understood within the context of exact three-body theory (alpha particle plus two nucleons,  $\alpha NN$ ) and good phenomenological representations of the low-energy behavior of the basic interactions ( $NN$  and  $\alpha N$ ). The most sophisticated models give  ${}^6\text{He}$  and  ${}^6\text{Li}$  three-body binding energies within 0.5 MeV of experiment,<sup>1</sup> predict a value for the  ${}^6\text{He}$   $\beta$ -decay rate within experimental errors,<sup>2</sup> and yield an impressive description of elastic and inelastic deuteron-alpha scattering.<sup>3</sup> Moreover, somewhat less complete models indicate that the  ${}^6\text{Li}$  charge radius and Coulomb energy,<sup>4</sup> the resonance structure of the  ${}^6\text{Li}$  low-lying excited states,<sup>5</sup> and the  ${}^6\text{Li}$  alpha-deuteron structure<sup>6</sup> can probably be understood through three-body physics. The purpose of this paper is to

present an extension of our earlier<sup>6</sup> work on the alpha-deuteron structure of  ${}^6\text{Li}$ , where now, the  ${}^6\text{Li} \rightarrow \alpha + d$  momentum distribution, percentage alpha-deuteron component, asymptotic normalization constants, and the effective alpha-deuteron wave function are calculated with our most complete  ${}^6\text{Li}$  three-body wave functions.<sup>1</sup> Thus, the  ${}^6\text{Li}$  alpha-deuteron structure predictions with three-body models now will be at the same level of sophistication as the  ${}^6\text{He}$   $\beta$  decay.<sup>2,7</sup>

In our earlier work<sup>6</sup> on the alpha-deuteron structure of  ${}^6\text{Li}$ , we used a simple three-body model where the triplet  $n$ - $p$  interaction was limited to  $s$  wave and the  $\alpha$ - $N$  interaction was represented by only the dominant  $P_{3/2}$  resonant part. This model is valuable as a first approximation in understanding bound-state properties, because it gives a value for the three-body binding energy essentially in agreement with experiment. Nevertheless, because

of its dynamical simplicity, important components in the wave function are missing and good agreement with experimental quantities such as  ${}^6\text{He}$   $\beta$  decay and asymptotic normalization constants cannot be expected. At best, it will yield results to within  $\sim 10\%$  for the latter two quantities, but these quantities are measured to within a few percent and thus can be used to discriminate 10% differences. Moreover, the very small and sensitive  $d$ -wave component of the alpha-deuteron structural quantities demands inclusion of the tensor component of the triplet  $n$ - $p$  interaction and the remaining significant components of the  $\alpha$ - $N$  interaction ( $S_{1/2}$  and  $P_{1/2}$  waves). Yet, this simple model has been valuable in interpreting the early data on the  ${}^6\text{Li} \rightarrow \alpha + d$  momentum distribution extracted from  ${}^6\text{Li}(p, pd)\alpha$  measurements,<sup>6</sup> the more recent  ${}^6\text{Li}(p, pd)\alpha$  results,<sup>8</sup> and  ${}^6\text{Li}(e, e'd)\alpha$  experiments.<sup>9</sup> Lately,<sup>10</sup> it has been used to study the important question concerning contraction of the deuteron cluster in  ${}^6\text{Li}$ .

On the basis of the model described in the previous paragraph, hereafter called the *simple* model, the alpha-deuteron ( $s$ -wave) properties of  ${}^6\text{Li}$  are predicted as follows: (1) The  $S$ -wave  ${}^6\text{Li} \rightarrow \alpha + d$  asymptotic normalization constant is 2.39, consistent with the experimentally determined value of  $\approx 2.4$  at the time,<sup>6</sup> but  $\sim 10\%$  higher than the current experimental value; (2) the  $d$ - $\alpha$  component of the three-body  ${}^6\text{Li}$  wave function is 65%, consistent with a dispersion *estimate* of 54% by Noble,<sup>11</sup> and lower than most experimental analyses at that time<sup>6</sup>; and (3) the  $d$ - $\alpha$  momentum distribution is consistent in shape and absolute magnitude with experiment.<sup>6,8,9</sup> The later work of Bang and Gignoux<sup>4</sup> supports the conclusion that the  $d$ - $\alpha$  component makes up about 50–60% of the  ${}^6\text{Li}$  wave function with their result of 52%. Thus, in first approximation, the predictions are in qualitative agreement with experiment and some of the physics has been extracted, but now experimental results have improved such that it is appropriate to extend the three-body model to test it further.

In the present work, we consider three models for comparison purposes: (1) simple, (2) full (0%), and (3) full (4%). The simple model is the one described above and used in our previous work. The full model includes the  $S_{1/2}$  and  $P_{1/2}$  waves of the  $\alpha$ - $N$

interaction (added to the dominant  $P_{3/2}$  wave of the simple model) and the triplet  $n$ - $p$  interaction is generalized to accommodate the tensor component. The amount of tensor component is characterized by the percentage of  $D$  state present in the deuteron: 0% or 4%. We emphasize comparisons of the model predictions with the latest experimental results for the  ${}^6\text{Li} \rightarrow \alpha + d$  momentum distribution, the  $S$ - and  $D$ -wave asymptotic normalization constants, and the percentage of  $s$ - and  $d$ -wave  $\alpha$ - $d$  component. In conjunction, the  $s$ - and  $d$ -wave effective configuration-space alpha-deuteron wave functions are given and discussed. All the  $d$ -wave alpha-deuteron results represent the first predictions of these quantities in parameter-free models beginning from the basic interactions required in the three-body dynamics.

The text is arranged as follows: Section II contains the theoretical framework from which the alpha-deuteron quantities are calculated. In Sec. III, the form of the  ${}^6\text{Li}$  wave function is explicitly given along with a detailed description of the three models used in this work. The results and discussion are presented in Sec. IV. Our conclusions are listed in Sec. V. Finally, an appendix gives the explicit equations used to calculate the various alpha-deuteron properties.

## II. THEORETICAL FRAMEWORK

The key quantity in the study of  ${}^6\text{Li}$  alpha-deuteron structure is the overlap amplitude of the  ${}^6\text{Li}$  ground state with a state for the  $\alpha$  particle and deuteron moving relative to each other with momentum  $\vec{q}$ . Specifically,

$$\begin{aligned} \langle \alpha d; \vec{q}, 1m_d | {}^6\text{Li}; 1m_6 \rangle \\ = \sum_{\substack{lm_l \\ (l \neq 1)}} f_l(q) \langle lm_l 1m_6 | 1m_d \rangle \sqrt{4\pi} Y_{m_l}^{[l]}(\hat{q}), \end{aligned} \quad (1)$$

where the  $m_i$  represent magnetic quantum numbers, the Clebsch-Gordan coefficient is defined as in Edmonds,<sup>12</sup> the spherical harmonics are defined in Ref. 1, and the square of  $f_l(q)$  is the  $l$ -wave  $\alpha$ - $d$  momentum distribution. The effective  $\alpha$ - $d$  configuration-space wave function is obtained from the Fourier transform of Eq. (1):

$$\langle \alpha d; \vec{\rho}, 1m_d | {}^6\text{Li}; 1m_6 \rangle = (2\pi)^{-3/2} \int d^3q e^{i\vec{q} \cdot \vec{\rho}} \langle \alpha d; \vec{q}, 1m_d | {}^6\text{Li}; 1m_6 \rangle \quad (2)$$

$$= \sum_{\substack{lm_l \\ (l \neq 1)}} i^l u_l(\rho) \langle lm_l 1m_6 | 1m_d \rangle \sqrt{4\pi} Y_{m_l}^{[l]}(\hat{\rho}), \quad (3)$$

where  $\vec{\rho}$  points from the  $\alpha$  particle to the deuteron center of mass and is conjugate to  $\vec{q}$ , while  $u_l(\rho)$  is defined to be the  $l$ -wave effective alpha-deuteron wave function and is given by

$$u_l(\rho) = \left[ \frac{2}{\pi} \right]^{1/2} \int_0^\infty q^2 dq j_l(q\rho) f_l(q). \quad (4)$$

Now, if we exploit the fact that the nearest singularity in the complex- $q$  plane of  $f_l(q)$  occurs at  $i\mu$ , where  $\mu = \sqrt{2\mu_{\alpha d} B_{\alpha d}}$  ( $\mu_{\alpha d}$  is the alpha-deuteron reduced mass and  $B_{\alpha d}$  is the binding energy of the alpha to the deuteron in  ${}^6\text{Li}$ ), we can derive

$$\lim_{\rho \rightarrow \infty} u_0(\rho) \rightarrow C_0^{\alpha d} \left[ \frac{\mu}{2\pi} \right]^{1/2} \frac{e^{-\mu\rho}}{\rho}, \quad (5)$$

$$\begin{aligned} \lim_{\rho \rightarrow \infty} \Psi_{m_6}^{[1]}(\vec{r}, \vec{\rho}) &\rightarrow C_0^{\alpha d} \left[ \frac{\mu}{2\pi} \right]^{1/2} \frac{e^{-\mu\rho}}{\rho} {}_d\Phi_{m_6}^{[1]}(\vec{r}) \\ &- C_2^{\alpha d} \left[ \frac{\mu}{2\pi} \right]^{1/2} \frac{e^{-\mu\rho}}{\rho} \left[ 1 + \frac{3}{\mu\rho} + \frac{3}{\mu^2\rho^2} \right] \sqrt{4\pi} [Y^{[2]}(\hat{\rho}) \times {}_d\Phi^{[1]}(\vec{r})]_{m_6}^{[1]}, \end{aligned} \quad (8)$$

where the minus sign in front of  $C_2^{\alpha d}$  arises because  $Y_m^{[2]}(\hat{\rho}) = i^2 Y_{2m}(\hat{\rho})$  and  $\vec{r}$  is the relative coordinate of the two nucleons. Therefore, we have defined the  $\alpha$ - $d$  momentum distributions, effective configuration-space wave functions, and asymptotic normalization constants. The final quantity of interest is the percentage (or fraction)  $\alpha$ - $d$  component which follows from the normalization of the  ${}^6\text{Li}$  wave function to unity with the insertion of the complete set of states

$$\sum_{m_d} \int d^3q |1m_d, \vec{q}; \alpha d\rangle \langle \alpha d; \vec{q}, 1m_d| + \sum_{S m_s} \int d^3q d^3k |Sm_s, \vec{q}; \alpha(np)_{\vec{k}}^s\rangle \langle \alpha(np)_{\vec{k}}^s; \vec{q}, Sm_s| = 1. \quad (9)$$

The result is

$$P_l^{\alpha d} = \int d^3q (f_l(q))^2, \quad (10)$$

that is, the fraction of  $l$ -wave  $\alpha$ - $d$  component in the  ${}^6\text{Li}$  wave function is the integral of the  $l$ -wave momentum distribution.

Of the four quantities defined above, three can be related to existing experiments. The  $\alpha$ - $d$  asymptotic normalization constants are extracted from dispersion-relation analyses of forward-angle elastic alpha-deuteron scattering, since they are related to the residues at the  ${}^6\text{Li}$  pole of the scattering amplitude, and the  ${}^6\text{Li}$ -pole term dominates such analyses.<sup>13</sup> The momentum distributions are obtained from coincidence experiments<sup>8,14,15</sup> like  ${}^6\text{Li}(p, p\alpha)d$ ,  ${}^6\text{Li}(\alpha, 2\alpha)d$ , or  ${}^6\text{Li}(p, pd)\alpha$ , and if the data covers a large enough range of  $q$  can be used to estimate<sup>16,17</sup> the  $P_l^{\alpha d}$ . It should be stressed that only the  $(p, p\alpha)$  and  $(\alpha, 2\alpha)$  cross sections factor into a product containing a kinematic factor, the  $p$ - $\alpha$  or  $\alpha$ - $\alpha$  cross section, and the sum of  $s$ - and  $d$ -wave momentum dis-

$$\lim_{\rho \rightarrow \infty} u_2(\rho) \rightarrow C_2^{\alpha d} \left[ \frac{\mu}{2\pi} \right]^{1/2} \frac{e^{-\mu\rho}}{\rho} \left[ 1 + \frac{3}{\mu\rho} + \frac{3}{\mu^2\rho^2} \right], \quad (6)$$

where the  $\alpha$ - $d$   $L$ -wave asymptotic normalization constants  $C_L^{\alpha d}$  are defined as

$$C_L^{\alpha d} \equiv i^L 2\pi i \mu^{1/2} \lim_{q \rightarrow i\mu} (q - i\mu) f_L(q). \quad (7)$$

This latter definition of the  $C_L^{\alpha d}$  is equivalent to the definition given directly from a  ${}^6\text{Li}$  three-body wave function; namely,

tributions, when the PWIA (DWIA) or (equivalently) exchange-pole dominance is assumed. The  $(p, pd)$  cross section factors only if the  $d$ -wave overlap amplitude is neglected.<sup>6</sup> Fortunately, the latter is a very good approximation since  $f_2(q)$  is very small compared to  $f_0(q)$  for a wide range of  $q$ . The  $(p, pd)$  cross section fails to factor in the presence of  $f_2(q)$  owing to the unit angular momentum of the exchanged deuteron. For completeness, we give the cross-section expressions:  $(p, p\alpha)$  [similarly for  $(\alpha, 2\alpha)$ ]

$$\frac{d^3\sigma}{d\Omega_p dE_p d\Omega_\alpha} = \frac{d\sigma(p\alpha)}{d\Omega_{\text{c.m.}}} \bar{\rho}(q) \text{ (kinematic factor)}, \quad (11)$$

where

$$\bar{\rho}(q) = \sum_{\substack{l=0 \\ l \neq 1}}^2 (f_l(q))^2, \quad (12)$$

but  $(p, pd)$

$$\frac{d^3\sigma}{d\Omega_p dE_p d\Omega_d} \approx \frac{d\sigma(pd)}{d\Omega_{\text{c.m.}}} (f_0(q))^2 \text{ (k.f.)}. \quad (13)$$

### III. MODELS EMPLOYED

The  ${}^6\text{Li}(1^+)$ , isospin singlet, wave function used in our work has the form

$$\Psi_{m_6}^{[1]}(\vec{k}_{12}, \vec{p}_3) = \frac{4\pi N}{K^2 + k_{12}^2 + \frac{3}{8}p_3^2} \left[ \lambda_1 \sum_{\substack{l,l'=0 \\ l,l' \neq 1}}^2 g_l^1(k_{12}) [[Y^{[l]}(\hat{k}_{12}) \times \chi^{[1]}(12)]^{[1]} \times Y^{[l']}(\hat{p}_3)]_{m_6}^{[1]} G^{l'}(p_3) \right. \\ \left. + \frac{5}{8} \sum_{J=1/2}^{3/2} \sum_{J'=|1-J|}^{1+J} \sum_{\substack{l=J-1/2 \\ l \leq 1}}^{J+1/2} \sum_{l'=J-1/2}^{J'+1/2} P^{l+l'} \Lambda_l^J \right. \\ \left. \times \{ h_l^J(k_{23}) F_{l'(J)}^{J'}(p_1) [\mathcal{Y}_{l'1/2}^{[J]}(\hat{k}_{23}, 2) \times \mathcal{Y}_{l'1/2}^{[J']}(\hat{p}_1, 1)]_{m_6}^{[1]} + (-1)^l (23, 1 \rightarrow 31, 2) \} \right], \quad (14)$$

where  $N$  is the normalization constant,  $P^L = \frac{1}{2}[1 + (-1)^L]$ , and the isospin function is suppressed. The spectator function  $G^l(p)$  gives the  $l$ -wave momentum distribution of the  $\alpha$  particle relative to the two-nucleon center of mass, while  $F_{l'(J)}^{J'}(p)$  gives the total angular-momentum  $J'$ —orbital-angular-momentum  $l'$  momentum distribution of a nucleon relative to the center of mass of an  $\alpha$ - $N$  pair interacting in the state  $l_J$ . There are nine spectator functions in the full model: two  $G$ 's and seven  $F$ 's. The form factors  $g_l^1(k)$  and  $h_l^J(k)$  in Eq. (14) originate from the separable potentials representing the  $NN$  and  $\alpha N$  interactions, respectively. These interactions have the forms

$$\langle \vec{k} | V_{NN} | \vec{k}' \rangle = -\frac{4\pi\lambda_1}{2\mu} \hat{1} \sum_{\substack{l,l'=0 \\ l,l' \neq 1}}^2 g_l^1(k) g_{l'}^1(k') [[Y^{[l]}(\hat{k}) \times \chi^{[1]}(12)]^{[1]} \times [Y^{[l']}(\hat{k}') \times \tilde{\chi}^{[1]}(12)]^{[1]}]^{[0]}, \quad (15)$$

where  $\mu$  is the  $NN$  reduced mass and  $\lambda_1$  is the triplet coupling strength;

$$\langle \vec{k} | V_{\alpha N} | \vec{k}' \rangle = -\frac{4\pi}{2\mu'} \sum_{J=1/2}^{3/2} \sum_{\substack{l=J-1/2 \\ l \leq 1}}^{J+1/2} \Lambda_l^J \hat{J} (-1)^{2J} h_l^J(k) h_l^J(k') [\mathcal{Y}_{l'1/2}^{[J]}(\hat{k}) \times \tilde{\mathcal{Y}}_{l'1/2}^{[J]}(\hat{k}')]^{[0]}, \quad (16)$$

where  $\mu'$  is the  $\alpha N$  reduced mass and  $\Lambda_l^J$  is the interaction strength for partial wave  $l$  and total angular momentum  $J$ . Thus in the full (4%) model, the  ${}^6\text{Li}$  wave function is generated from the  ${}^3S_1$ - ${}^3D_1$   $NN$  interactions and the  $S_{1/2}$ ,  $P_{1/2}$ , and  $P_{3/2}$   $\alpha N$  interactions. The details of calculating the wave function along with a complete discussion of the interaction parameters can be found in Ref. 1.

As mentioned in Sec. I, we consider three models in the present work: simple, full (0%), and full (4%). In Table I, we give the model binding energies ( $K^2/M$ ) along with the reference in which can be found the detailed form of the spectator functions and the values of  $N$ .<sup>18</sup> An appendix to this paper gives detailed expressions for calculating the  $f_l(q)$  and  $C_L^{ad}$  that can be derived from the wave function form of Eq. (14).

### IV. RESULTS AND DISCUSSION

We begin this section by considering the  ${}^6\text{Li} \rightarrow \alpha + d$  momentum distribution. In Fig. 1, we present the three-body predictions for the full (4%)

(solid curve) and the simple (long-dashed curve) models compared to the data available at the time of our earlier work.<sup>6</sup> The data represent the momentum distribution as extracted from two  ${}^6\text{Li}(p, pd)\alpha$  experiments: one at 155 MeV incident proton energy<sup>14</sup> (open circles) and the other at 590 MeV.<sup>15</sup> The data both indicate consistency as far as absolute magnitude near  $q=0$ , but the 590 MeV data imply a wider distribution, i.e., a greater full width at half maximum (FWHM). In fact, the simple model seems to be in better agreement with the

TABLE I. Model binding energies.

Model <sup>a</sup>	Binding energy <sup>b</sup> (MeV)	Ref.
Simple	4.660	6
Full (0%)	4.446	1
Full (4%)	4.062	1

<sup>a</sup>The quantity in parentheses is the percentage  $D$  state in the deuteron for the  ${}^3S_1$ - ${}^3D_1$  interaction used to generate the  ${}^6\text{Li}$  wave function.

<sup>b</sup>The experimental binding energy for  ${}^6\text{Li}$  is 4.531 [3.697 + 0.834 (Coulomb)] MeV.

data than the full (4%) model. However, a recent reanalysis<sup>19</sup> of the 590 MeV experiment suggests that the FWHM should be reduced by  $\sim 60\%$ . Such a narrowing of the distribution clearly favors the full (4%) model. Consistent with the reanalysis of the 590 MeV data is the new data at 670 MeV shown in Fig. 2 along with the full (4%)-model curve. All three sets of data are in agreement about the absolute magnitude of the momentum distribution near  $q=0$ , implying that absorption effects are not large over the energy range indicated. Moreover, the full (4%) model agrees very well with the 670 MeV data over the expected range of validity of a pole-dominance (or PWIA) analysis, specifically  $q \lesssim 0.3 \text{ fm}^{-1}$ . Albrecht *et al.*<sup>8</sup> have pointed out, and Erö has reiterated to us,<sup>20</sup> that deviations from the three-body predictions are possible on the basis that the  $p$ - $d$  cross section for the elementary quasi-free scattering, that which should be used in Eq. (13), is larger than the *free*  $p$ - $d$  scattering cross section used in the extraction of  $\bar{\rho}(q)$ . This would be a consequence of the large-angle scattering geometry used in the 670 MeV experiment. At backward angles, a virtual-pion-exchange mechanism<sup>21</sup> appears to have a dominating role in the  $p$ - $d$  scattering near

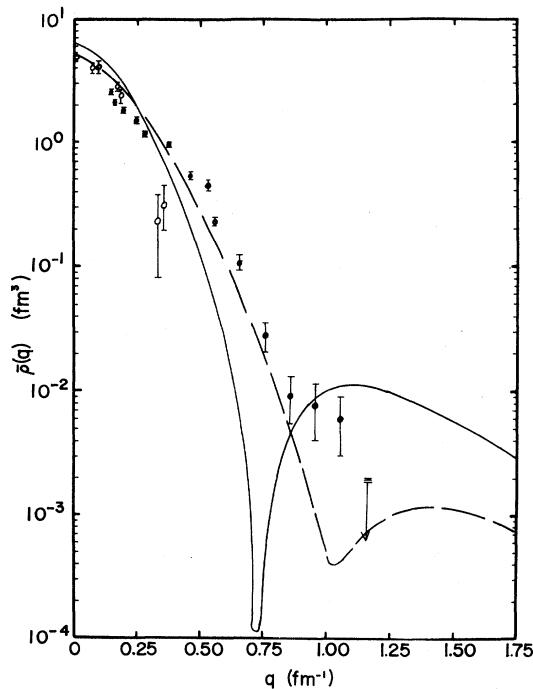


FIG. 1.  ${}^6\text{Li} \rightarrow \alpha + d$  momentum distribution. The data are extracted from  ${}^6\text{Li}(p, pd)\alpha$  experiments at 155 MeV (open circles, Ref. 14) and 590 MeV (solid circles, Ref. 15). The theoretical curves are the full (4%) (solid line) and simple (long-dashed line) models.

670 MeV and this mechanism is sensitive to the actual form of the  $n$ - $p$  relative wave function. Deformation of the deuteron cluster might be reflected in the elementary  $p$ - $d$  cross section.<sup>10</sup> Possibly, this is the source of the underestimation of the momentum distribution by the full (4%) model for  $q > 0.3 \text{ fm}^{-1}$ . Clearly, it would be valuable to perform a calculation that checks the role of the virtual-pion-exchange mechanism in the analysis of the 670 MeV data,<sup>22</sup> but on the whole, the full (4%) model agrees very well with the low- $q$  experimental momentum distribution.

Returning to Fig. 1, we note that the momentum distributions predicted by the simple and full (4%) models are quite distinct, whereas the differences between the full (0%) and full (4%) are relatively small, as can be seen in Fig. 3. The presence of the tensor force leads to a higher value of  $\bar{\rho}(0)$  (see Table II) and a deeper diffraction minimum that occurs at a somewhat smaller  $q$  value ( $\sim 0.725 \text{ fm}^{-1}$  as opposed to  $\sim 0.775 \text{ fm}^{-1}$ ). The diffraction minimum is an interesting feature of all three models and reflects the role of the Pauli exclusion

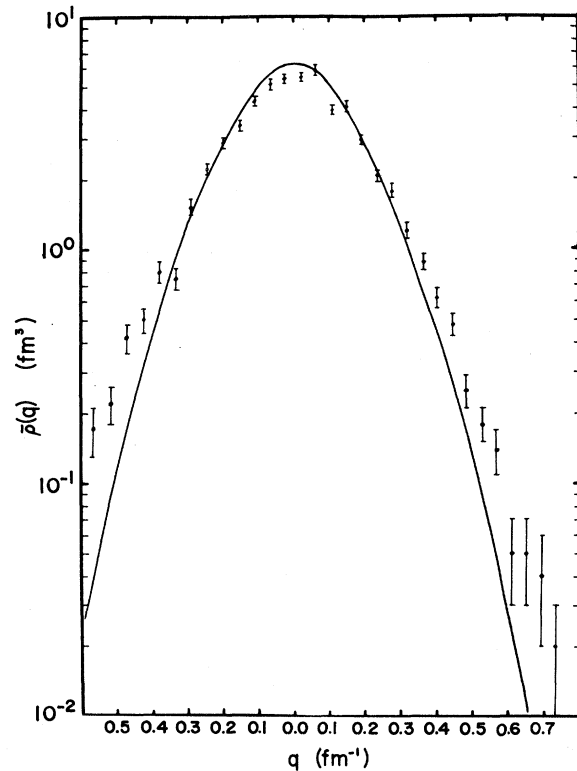


FIG. 2.  ${}^6\text{Li} \rightarrow \alpha + d$  momentum distribution. The data are extracted from a  ${}^6\text{Li}(p, pd)\alpha$  experiment at 670 MeV (Ref. 8) corrected for finite angular and energy resolution by Monte Carlo calculation (Ref. 20). The theoretical curve is the full (4%) model.

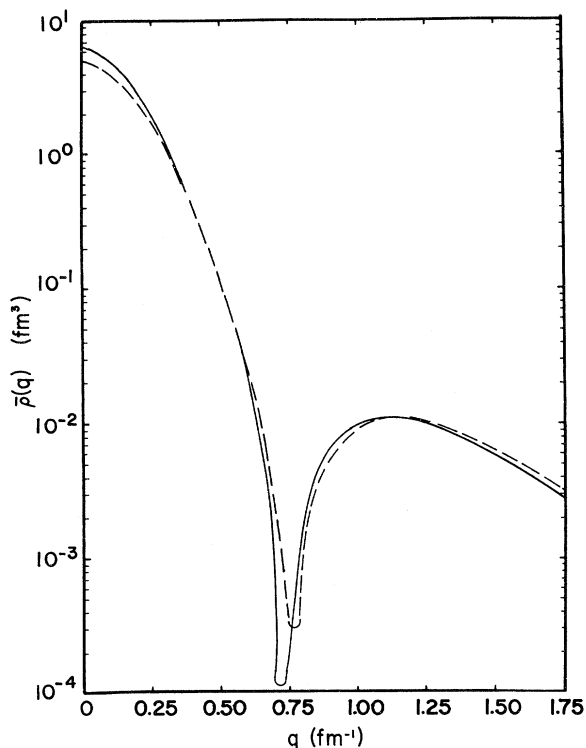


FIG. 3. Comparison of the  ${}^6\text{Li} \rightarrow \alpha + d$  momentum distributions from the (0%) (short-dashed line) and full (4%) (solid line) models.

principle, i.e., two valence nucleons outside closed shells (the  $\alpha$  particle). The location of the minimum is markedly different for the simple and full (4%) models. The full (4%) model minimum occurs more than  $0.25 \text{ fm}^{-1}$  before the one of the simple model, a direct consequence of the *repulsive*  $S_{1/2}$   $\alpha$ - $N$  interaction being present in the full models. Such a distinct feature with its depth and location predicted is worth attempting to verify experimentally, especially since it occurs within the expected range of validity of the three-body model, namely  $q \lesssim 0.9 \text{ fm}^{-1}$ . Clearly, such a measurement

TABLE II. Predicted momentum distribution properties.

Model	$\bar{\rho}(0)$ ( $\text{fm}^3$ )	$q_{\min}$ ( $\text{fm}^{-1}$ ) <sup>a</sup>	FWHM (MeV/ $c$ )
Simple	4.859	1.025	$\sim 80.5$
Full (0%)	4.947	0.775	$\sim 77.0$
Full (4%)	6.309	0.725	$\sim 75.0$

<sup>a</sup>Momentum transfer at  ${}^6\text{Li}$  vertex where diffraction minimum occurs.

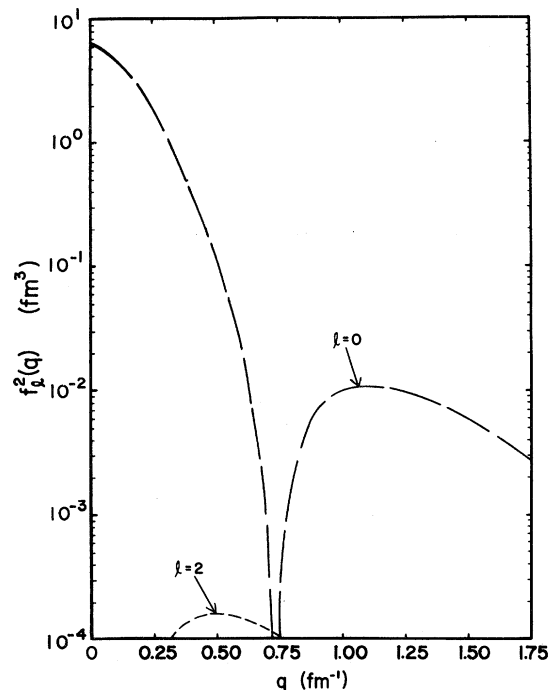


FIG. 4. Partial-wave contributions to the  ${}^6\text{Li} \rightarrow \alpha + d$  momentum distribution for the full (4%) model.

requires a high resolution (in  $q$ ) experiment and is probably best done with electrons where distortion effects are not a problem.<sup>23</sup> Moreover, the theoretical analysis would be optimal for the more difficult  ${}^6\text{Li}(e, e'\alpha)d$  arrangement, but  ${}^6\text{Li}(e, e'd)\alpha$  would be just as valuable.

The last sentence of the previous paragraph goes back to the point about factorization of the coincidence cross section for  $\alpha$ 's detected in coincidence, but not for deuterons (see the last paragraph of Sec. II). In Figs. 1 and 2, we have labeled the ordinate as  $\bar{\rho}(q)$ , but strictly speaking for a  ${}^6\text{Li}(p, pd)\alpha$  experiment to have the standard factorization an approximation is employed:

$$\bar{\rho}(q) \approx (f_0(q))^2, \quad (17)$$

i.e., the  $d$ -wave overlap amplitude is neglected. Nonetheless, since  $f_2(q)$  is so small, we did plot  $\bar{\rho}(q)$  for the theoretical curves. Figure 4 displays the two momentum distributions separately and makes it clear that the diffraction minimum occurs in the  $s$ -wave distribution (as you would expect on the basis of Pauli principle arguments) and it is filled in somewhat by the  $d$ -wave distribution. Therefore, except in the vicinity of the diffraction minimum, the three-body model predicts that one is justified in neglecting  $f_2(q)$ .

Directly linked to the  ${}^6\text{Li} \rightarrow \alpha + d$  momentum distributions is the fraction or percentage  $\alpha$ - $d$  component in the  ${}^6\text{Li}$  wave functions [see Eq. (10) above]. In Table III, we list the three-body model results broken apart according to partial wave. Three features stand out: (1) All three models predict  $\sim 63$ – $66\%$   $\alpha$ - $d$  component in the  ${}^6\text{Li}$  wave function; (2) all three models predict that the  $l=2$   $\alpha$ - $d$  component is  $< 1\%$ ; and (3) the presence of the  $n$ - $p$  tensor force dramatically reduces the  $l=2$  component by almost a factor of 6 to  $\sim 0.05\%$ . Significantly, all three models are consistent with the latest attempts at extracting the percentage  $\alpha$ - $d$  component from experiment. One feature of interest in Table III is the last theoretical entry labeled full (4%  $t=0$ ) which is obtained by setting  $g_2^1(k) \equiv 0$  in the full (4%) wave function, renormalizing the wave function to unity, and recalculating the results. It indicates that the tensor-force terms contribute  $\sim 3\%$  to the  $s$ -wave  $\alpha$ - $d$  component and  $\sim 50\%$  of the  $d$ -wave component. The  $d$ -wave results given in Table III constitute the first predictions of this quantity from a full dynamical model, but Noble's phenomenological estimate<sup>24</sup> of 0.027% differs by only a factor of 2 with the full (4%) prediction. As pointed out by Noble, shell-model calculations exist that predict 0.08%  $d$ -wave component<sup>25</sup> and 9%  $d$ -wave component.<sup>26</sup> The latter seems to be clearly ruled out. Qualitatively, it appears that the result of  $\sim 0.05\%$  for the  $d$ -wave  $\alpha$ - $d$  component is a consequence of the reduced role of the deuteron  $s$ -wave wave function component in the structure (binding) of the deuteron when the tensor force is present. The latter is reflected in a slightly smaller inverse-range parameter in the  $s$ -wave form factor [ $g_0^1(k)$ ] and a 38% reduction in the (effective)  $s$ -wave strength parameter of the potential.<sup>1</sup> Comparison of the full (0%) and full (4%  $t=0$ ) results supports this interpretation.

We turn now to the components of the effective

TABLE III. Percentage alpha-deuteron component.

Model	$P_0^{ad}$	$P_2^{ad}$	$P_{\text{total}}^{ad}$
Simple	64.9	0.63	65.5
Full (0%)	63.2	0.28	63.5
Full (4%)	65.4	0.049	65.4
Full (4% $t=0$ )	62.1	0.025	62.1
Experimental values			$58 \pm 9^a$ $52 \pm 13^b$

<sup>a</sup>Reference 16.

<sup>b</sup>Reference 17.

alpha-deuteron wave function which are defined as the Fourier transform of the overlap amplitudes, Eq. (4).<sup>27</sup> The  $s$ -wave component is displayed in Fig. 5 for all three models. As expected from the momentum distributions, the simple model gives markedly different results from the full models and the presence of the tensor force does not lead to a significant change from the full (0%) curve. All models lead to the expected  $2s$  shape required by the Pauli principle, but the presence of the  $S_{1/2}$   $\alpha$ - $N$  interaction makes the inner lobe more significant and thus moves the node farther from the origin ( $\sim 1.6$  fm) in the full models. Far more contrast exists between models for the  $d$ -wave wave function as can be seen in Fig. 6. The presence of the tensor force causes a node to be present; otherwise, no node is predicted. Unlike Noble's assumption,<sup>24</sup> the three-body model does not predict that the  $s$ - and  $d$ -wave effective alpha-deuteron wave functions have the same shape, even though for the full (4%) model they have similar nodal behavior. The role of the explicitly tensor-force contributions can be seen in Figs. 7 and 8, where we have compared the full (4%) model with the full (4%  $t=0$ ) model. As expected on the basis of the  $P_1^{ad}$  results, the  $d$ -wave wave function is most changed by their removal—the inner lobe is smaller and the node closer to the origin when the explicit tensor-force terms are present.

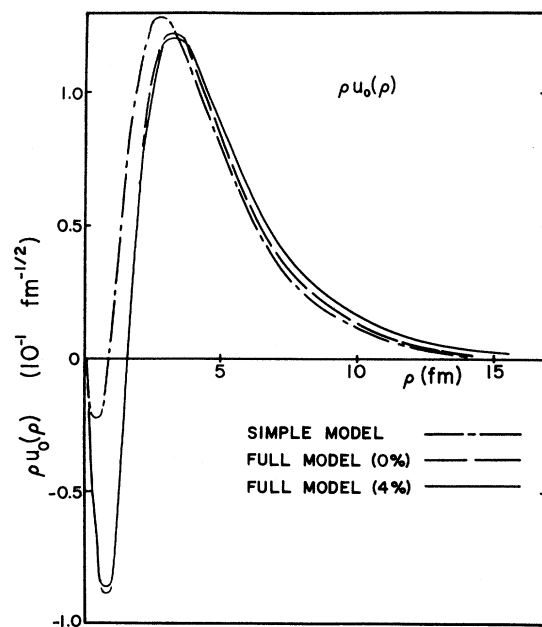


FIG. 5. Effective  $\alpha$ - $d$   $s$ -wave wave function. Comparison of three-body models.

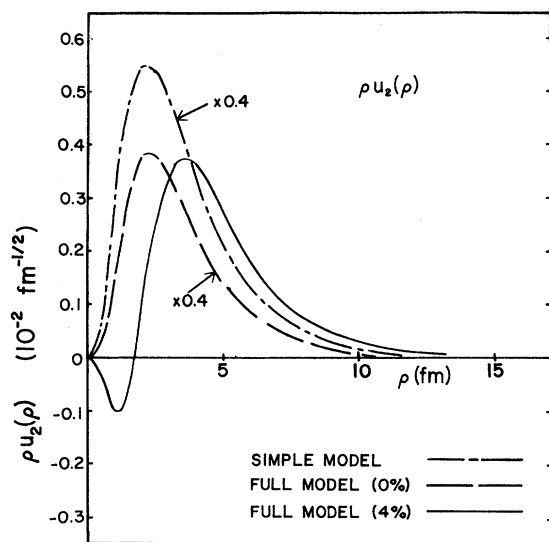


FIG. 6. Effective  $\alpha$ - $d$   $d$ -wave wave function. Comparison of three-body models.

Returning once again to the  $s$ -wave wave function, it is interesting to compare the full (4%) model with a  $2s$  pure  $\alpha$ - $d$  cluster ( $\alpha$  and  $d$  elementary particles) model derived from a Woods-Saxon potential adjusted to produce the experimental  $\alpha$ - $d$  binding energy.<sup>28</sup> When they are normalized on the same scale, their shapes are almost identical (see Fig. 9). Band and Gignoux found a similar result.<sup>4</sup> This re-

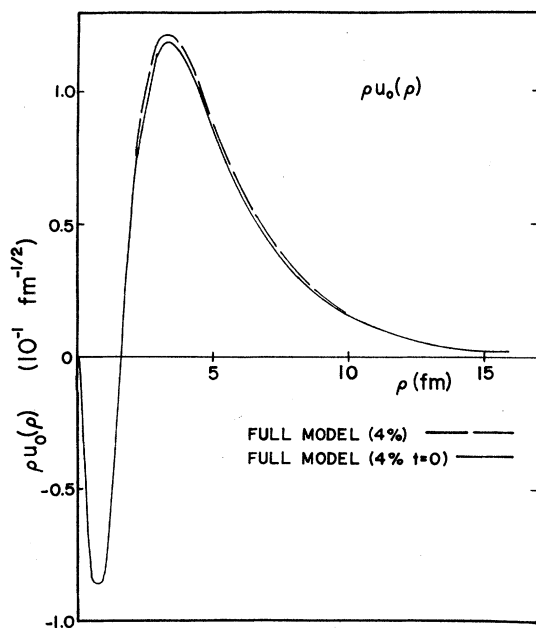


FIG. 7. Effective  $\alpha$ - $d$   $s$ -wave wave function. Effect of explicit tensor-force terms.

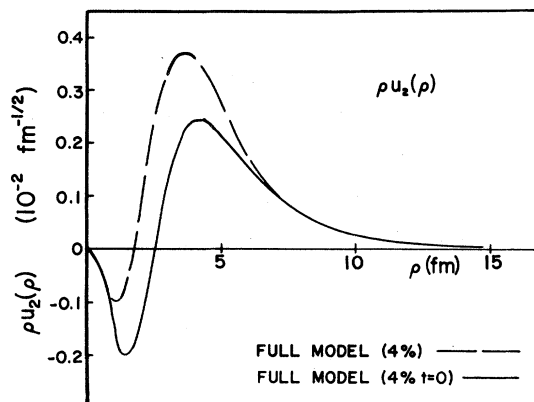


FIG. 8. Effective  $\alpha$ - $d$   $d$ -wave wave function. Effect of explicit tensor-force terms.

sult suggests that a Woods-Saxon  $2s$  wave function normalized to  $P_0^{ad}$  gives a good representation of the  $\alpha$ - $d$  relative motion provided the process under consideration is not sensitive to the fact that the deuteron is not an elementary particle.

The final alpha-deuteron structural quantities that we consider are the  ${}^6\text{Li} \rightarrow \alpha + d$  asymptotic normalization constants. The three-body predictions are given in Table IV along with the latest experimental values. Again, the reader should note several points: (1) For the  $S$ -wave asymptotic normalization constant, only the full (4%) value falls

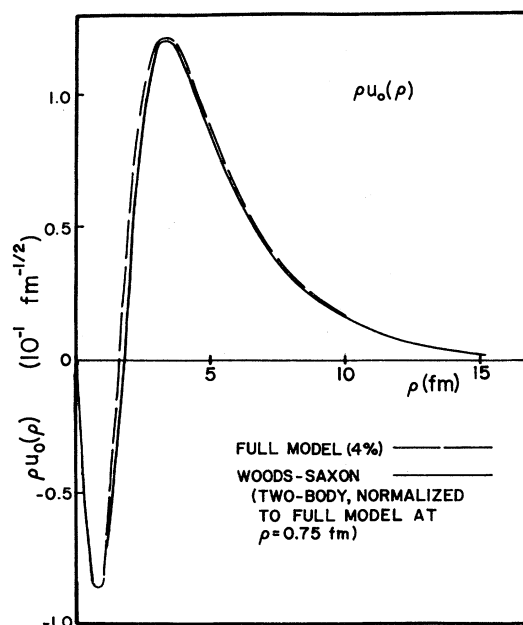


FIG. 9. Effective  $\alpha$ - $d$   $s$ -wave wave function. Comparison of pure cluster model form with three-body prediction.

TABLE IV. Asymptotic normalization constants.

Model	$C_0^{\alpha d}$	$C_2^{\alpha d}$
Simple	2.391	0.0545
Full (0%)	2.321	0.0286
Full (4%)	2.182	0.0178
Full (4% $t=0$ )	2.206	-0.00004
Experimental value <sup>a</sup>	$2.15 \pm 0.05$	$0.01 \pm 0.03$

<sup>a</sup>See Ref. 13.

within experimental errors, a situation that is identical to our  $\beta$ -decay predictions.<sup>2</sup> (2) Only the full model predicts  $D$ -wave asymptotic norm values consistent with experiment, but unfortunately the experimental value is not known well enough to distinguish between the full (0%) and full (4%) models, or for that matter, to even specify the sign. (3) The three-body models considered predict that the  $D$ -wave asymptotic norm is *positive* relative to the  $S$  wave, a striking prediction since the phenomenological pure  $\alpha$ - $d$  cluster model requires a negative sign in order to have the proper sign for the  ${}^6\text{Li}$  quadrupole moment.<sup>24</sup> (4) The contributions from the explicit tensor-force terms are small for the  $S$ -wave asymptotic norm, but critical in leading to the sign and magnitude of the  $D$  wave [compare full (4%) with full (4%  $t=0$ )]. Since the  $D$ -wave asymptotic norm depends on and is sensitive to the small components of the  ${}^6\text{Li}$  wave function, it provides a good test of the three-body model. It would be valuable to find a method whereby it can be measured more accurately and with good precision.<sup>29</sup>

Before closing this section, two comments should be made; one concerns neglect of the alpha-particle structure and the other pertains to Coulomb effects. A question that is frequently asked is "Why should binding energies and other properties of the  $A=6$  system not be sensitive to the structure of the alpha particle?" Perhaps, it will turn out that a three-body ( $\alpha NN$ ) model of the  $A=6$  system is inadequate for understanding *in detail* low-energy dynamics and properties. Nevertheless, a first step towards understanding the importance of the alpha-particle structure is to perform dynamically correct three-body calculations with the best available phenomenological  $\alpha$ - $N$  and  $N$ - $N$  interactions to look for discrepancies with experiment. Such effort is important, because calculations of the latter type take us beyond effective two-body theories, e.g., shell models,  $\alpha$ - $d$  cluster models, etc. Moreover, the present work plus earlier calculations<sup>1-3</sup> indi-

cate qualitative, if not quantitative, validity of the model within present experimental errors for those cases examined. At this stage, improvement of experimental results and theoretical calculations of other measurables ( ${}^6\text{Li}$  quadrupole moment, charge form factors, etc.) are needed before a conclusion about the shortcomings of three-body models can be reached. One aspect of the present calculations that should not be ignored is neglect of the Coulomb interaction—especially with respect to the asymptotic normalization constants.<sup>13</sup> Coulomb effects might be expected to modify results significantly since the Coulomb parameter (set up for  $\alpha$ - $d$ )

$$\kappa = \mu_{\alpha d} Z_{\alpha} Z_d e^2 / \hbar^2 \mu = 0.301 .$$

Nonetheless, one should be cautious since a combination of effects come into play that can compensate for each other. For example, the asymptotic  $\alpha$ - $d$  wave function at large distances now behaves as a Whittaker function which leads to a more rapid decrease with increasing  $\rho$  owing to the extra  $\rho^{-\kappa}$  factor, but this is compensated for by the decrease in binding energy that creates a slower falloff of the exponential factor. When these aspects are added to the change in the intermediate-range shape of the  $\alpha$ - $d$  wave function, it is difficult to predict how much different the asymptotic normalization constant values will be when Coulomb effects are included.<sup>30</sup> Future work on alpha-deuteron structure should address this issue.

## V. CONCLUSIONS

Both the  $s$ - and  $d$ -wave alpha-deuteron structural properties of  ${}^6\text{Li}$  were investigated within the framework of exact three-body theory ( $\alpha NN$ ) where the  ${}^3S_1$ - ${}^3D_1$   $n$ - $p$  and  $S_{1/2}$ ,  $P_{1/2}$ , and  $P_{3/2}$   $\alpha$ - $N$  interactions are the only input. Three models were considered: simple model—only the  ${}^3S_1$   $n$ - $p$  and resonant  $P_{3/2}$   $\alpha$ - $N$  interactions; full (0%) model— ${}^3S_1$   $n$ - $p$  and all three  $\alpha$ - $N$  interactions; and full (4%) model—same as the full (0%) model, but with the  ${}^3D_1$   $n$ - $p$  interaction included such that the deuteron has a 4%  $D$ -state component. Four alpha-deuteron quantities were examined: (1)  ${}^6\text{Li} \rightarrow \alpha + d$  momentum distribution; (2) percentage  $\alpha$ - $d$  component in the  ${}^6\text{Li}$  wave function; (3) form of the configuration-space  $\alpha$ - $d$  wave function; and (4) values of the  ${}^6\text{Li} \rightarrow \alpha + d$  asymptotic normalization constants. The major conclusions of this work are:

(1)  ${}^6\text{Li} \rightarrow \alpha + d$  momentum distribution: (a) For low momentum transfers ( $q \leq 0.3 \text{ fm}^{-1}$ ), the full (4%) model is in agreement with the data from the

most recent  ${}^6\text{Li}(p, pd)\alpha$  experiment at 670 MeV incident proton energy. (b) A diffraction minimum, whose source is the Pauli principle, is predicted to occur at  $q \sim 0.75 \text{ fm}^{-1}$ , and we suggest that it be looked for in  ${}^6\text{Li}(e, e'\alpha)d$  or  ${}^6\text{Li}(e, e'd)\alpha$  experiments. (c) The  $n$ - $p$  tensor force changes the predicted momentum distribution by a relatively small amount. (d) The  $d$ -wave component of the momentum distribution is so small that its main effect is to slightly fill in the diffraction minimum of the  $s$ -wave component.

(2) Percentage  $\alpha$ - $d$  component: All the three-body models considered predict that the  $\alpha$ - $d$  component of the  ${}^6\text{Li}$  wave function is  $\sim 65\%$ , consistent with the latest experimental determination. The full (4%) model predicts that the very sensitive  $d$ -wave contribution is only 0.049%.

(3) Effective  $\alpha$ - $d$  wave function: All three models predict that the  $s$ -wave component has a node, consistent with the Pauli principle, but the simple and

full models differ significantly in their location of the node. Both the full models locate the node at  $\sim 1.6 \text{ fm}$ . Predictions for the  $d$ -wave component differ for all three models; in particular, only the full (4%) model predicts a node in this wave function at  $\sim 1.65 \text{ fm}$ .

(4)  ${}^6\text{Li} \rightarrow \alpha + d$  asymptotic normalization constants: The  $S$ - and  $D$ -wave asymptotic norms are predicted to be 2.182 and 0.0178, respectively, from the full (4%) model. With a caveat concerning Coulomb effects, these predictions are consistent with the current experimental extraction.

#### ACKNOWLEDGMENTS

The authors would like to thank J. Erö for sending them the data points plotted in Fig. 2 and his comments about comparing theory with experiment. The work of D.R.L. was supported in part by the Department of Energy.

#### APPENDIX

In this appendix, we give the detailed form for the overlap amplitudes and asymptotic normalization constants as derived from Eqs. (14), (1), (7), and the deuteron wave function

$${}_d\psi_m^{[11]}(\vec{p}) = \frac{N_d \sqrt{4\pi} \sum_{\substack{l=0 \\ l \neq 1}}^2 g_l^1(p) [Y^{[1]}(\hat{p}) \times \chi^{[11]}(12)]_m^{[1]}}{p^2 + \gamma^2}, \quad (\text{A1})$$

where  $N_d$  is the normalization constant and the deuteron binding energy is  $\gamma^2/2\mu_{NN}$ . The overlap amplitudes are

$$\begin{aligned} f_0(q) = NN_d \left\{ \lambda_1 G^0(q) \int d^3k \frac{\sum_{\substack{l=0 \\ l \neq 1}}^2 (g_l^1(k))^2}{(k^2 + \gamma^2)(K^2 + k^2 + \frac{3}{8}q^2)} \right. \\ \left. + 2\pi \int_0^\infty k^2 dk \int_{-1}^1 d\xi \frac{1}{k^2 + \frac{q^2}{4} + \gamma^2 + kq\xi} \right. \\ \left. \times \left[ I_{00}^{1/2} F_{0(1/2,0)}^{1/2}(k) - \frac{1}{3} \left[ I_{01}^{1/2} (F_{1(1/2,1)}^{1/2}(k) - 2\sqrt{2} F_{1(1/2,1)}^{3/2}(k)) \right. \right. \right. \\ \left. \left. \left. + 2\sqrt{2} I_{01}^{3/2} \left[ F_{1(3/2,1)}^{1/2}(k) - \frac{\sqrt{5}}{2} F_{1(3/2,1)}^{3/2}(k) \right] \right] T_1 \right. \right. \\ \left. \left. - \frac{1}{2} I_{20}^{1/2} F_{2(1/2,0)}^{3/2}(k) T_2 + \frac{\sqrt{2}}{3} \left[ I_{21}^{1/2} \left[ F_{1(1/2,1)}^{1/2}(k) + \frac{1}{2\sqrt{2}} F_{1(1/2,1)}^{3/2}(k) \right] \right. \right. \right. \\ \left. \left. \left. - \frac{1}{2\sqrt{2}} I_{21}^{3/2} \left[ F_{1(3/2,1)}^{1/2}(k) + \frac{2}{\sqrt{5}} F_{1(3/2,1)}^{3/2}(k) \right] \right] \right. \right. \\ \left. \left. \times T_3 - \frac{3}{2\sqrt{5}} I_{21}^{3/2} F_{3(3/2,1)}^{5/2}(k) T_4 \right] \right\} \quad (\text{A2}) \end{aligned}$$

and

$$\begin{aligned}
f_2(q) = NN_d \left\{ \lambda_1 G^2(q) \int d^3k \frac{\sum_{\substack{l=0 \\ l \neq 1}}^2 (g_l^1(k))^2}{(k^2 + \gamma^2)(K^2 + k^2 + \frac{3}{8}q^2)} \right. \\
+ 2\pi \int_0^\infty k^2 dk \int_{-1}^1 d\xi \frac{1}{k^2 + \frac{q^2}{4} + \gamma^2 + kq\xi} \\
\times \left[ -\frac{1}{2} I_{00}^{1/2} F_{2(1/2,0)}^{3/2}(k) T_5 + \frac{\sqrt{2}}{3} \left[ I_{01}^{1/2} \left[ F_{1(1/2,1)}^{1/2}(k) + \frac{1}{2\sqrt{2}} F_{1(1/2,1)}^{3/2}(k) \right] \right. \right. \\
\left. \left. - \frac{1}{2\sqrt{2}} I_{01}^{3/2} \left[ F_{1(3/2,1)}^{1/2}(k) + \frac{2}{\sqrt{5}} F_{1(3/2,1)}^{3/2}(k) \right] \right] \right. \\
- \frac{3}{2\sqrt{5}} I_{01}^{3/2} F_{3(3/2,1)}^{5/2}(k) T_7 + \frac{1}{2} I_{20}^{1/2} \left[ F_{0(1/2,0)}^{1/2}(k) T_8 - \frac{1}{\sqrt{2}} F_{2(1/2,0)}^{3/2}(k) T_9 \right] \\
+ \frac{1}{2} I_{21}^{1/2} \left[ \frac{2}{5} F_{1(1/2,1)}^{1/2}(k) T_{10} + \frac{1}{\sqrt{2}} F_{1(1/2,1)}^{3/2}(k) T_{11} \right] \\
\left. + \frac{1}{2} I_{21}^{3/2} \left[ -\frac{1}{\sqrt{2}} F_{1(3/2,1)}^{1/2}(k) T_{12} + \frac{1}{15} \sqrt{2/5} F_{1(3/2,1)}^{3/2}(k) T_{13} - 3\sqrt{2/5} F_{3(3/2,1)}^{5/2}(k) T_{14} \right] \right\}, \quad (\text{A3})
\end{aligned}$$

where

$$\begin{aligned}
I_{lL}^J &\equiv I_{lL}^J(k, q, \xi; K^2) \\
&= \frac{5}{4} \Lambda_L^J \frac{\mathcal{G}_l^1(|\vec{k} + \frac{1}{2}\vec{q}|) \mathcal{H}_L^J(|\frac{4}{5}\vec{k} + \vec{q}|)}{K^2 + k^2 + \frac{5}{8}q^2 + kq\xi}, \quad (\text{A4})
\end{aligned}$$

$$\mathcal{G}_l^1(k) = g_l^1(k)/k^l, \quad (\text{A5})$$

$$\mathcal{H}_L^J(k) = h_L^J(k)/k^L, \quad (\text{A6})$$

$$T_1 = \frac{4}{5}k + q\xi, \quad (\text{A7})$$

$$T_2 = 2k^2 + \frac{q^2}{4}T_5 + 2kq\xi, \quad (\text{A8})$$

$$T_3 = \frac{8}{5}k^3 + \frac{18}{5}qk^2\xi + \frac{q^2k}{10}(13 + 11\xi^2) + \frac{q^3}{2}\xi, \quad (\text{A9})$$

$$T_4 = \frac{8}{5}k^3 + \frac{18}{5}qk^2\xi + \frac{6}{5}q^2kT_5 + \frac{q^3\xi}{4}(5\xi^2 - 3), \quad (\text{A10})$$

$$T_5 = 3\xi^2 - 1, \quad (\text{A11})$$

$$T_6 = \frac{4}{5}kT_5 + 2q\xi, \quad (\text{A12})$$

$$T_7 = \frac{4}{5}kT_5 + q\xi(5\xi^2 - 3), \quad (\text{A13})$$

$$T_8 = k^2T_5 + 2kq\xi + \frac{q^2}{2}, \quad (\text{A14})$$

$$T_9 = \left[ k^2 + \frac{q^2}{4} \right] T_5 + \frac{kq\xi}{2}(3\xi^2 + 1), \quad (\text{A15})$$

$$T_{10} = \frac{2}{3}k^3T_5 + k^2q\xi(2\xi^2 + 1) + \frac{kq^2}{12}(17\xi^2 + 7) + \frac{5}{12}q^3\xi, \quad (\text{A16})$$

$$T_{11} = \frac{4}{3}k^3T_5 + \frac{k^2q\xi}{5}(47\xi^2 - 17) + \frac{kq^2}{15}(83\xi^2 - 23) + \frac{5}{6}q^3\xi, \quad (\text{A17})$$

$$T_{12} = \frac{4}{3}k^3T_5 + \frac{2k^2q\xi}{5}(\xi^2 + 14) + \frac{kq^2}{30}(31\xi^2 + 89) + \frac{5}{6}q^3\xi, \quad (\text{A18})$$

$$T_{13} = 16k^3 T_5 + \frac{3}{2} k^2 q \xi (41\xi^2 + 7) + \frac{kq^2}{4} (163\xi^2 + 29) + 10q^3 \xi, \quad (\text{A19})$$

$$T_{14} = \frac{2}{5} k^3 T_5 + \frac{k^2 q \xi}{2} (13\xi^2 - 4) + \frac{kq^2}{4} (5\xi^4 + \frac{6}{5}\xi^2 - \frac{7}{5}) + \frac{q^3}{8} \xi (5\xi^2 - 3). \quad (\text{A20})$$

The asymptotic normalization constants are derived from the  $f_l(q)$  and the integral equations for the  $G^l(q)$  spectator functions. Then, from Eq. (7), we derive

$$C_L^{ad} = i^L \frac{8NN_d \pi}{3\mu^{1/2}} \mathcal{F}_L(i\mu), \quad (\text{A21})$$

where the  $\mathcal{F}_L(q)$  have the same form as the angle-dependent terms of the  $f_l(q)$ , but with the factor  $(k^2 + q^2/4 + kq\xi + \gamma^2)^{-1}$  removed; that is,

$$\mathcal{F}_0(q) = 2\pi \int_0^\infty k^2 dk \int_{-1}^1 d\xi (I_{00}^{1/2} F_{0(1/20)}^{1/2}(k) + \dots) \quad (\text{A22})$$

and

$$\mathcal{F}_2(q) = 2\pi \int_0^\infty k^2 dk \int_0^\infty d\xi (-\frac{1}{2} I_{00}^{1/2} F_{2(1/20)}^{3/2}(k) T_5 + \dots). \quad (\text{A23})$$

It is easy to prove that the  $C_L^{ad}$  are real.

- <sup>1</sup>A. Ghovanlou and D. R. Lehman, Phys. Rev. C **9**, 1730 (1974); D. R. Lehman, M. Rai, and A. Ghovanlou, *ibid.* **17**, 744 (1978). References to earlier work can be found in these papers.
- <sup>2</sup>W. C. Parke, A. Ghovanlou, C. T. Noguchi, M. Rajan, and D. R. Lehman, Phys. Lett. **74B**, 158 (1978).
- <sup>3</sup>Y. Koike, Prog. Theor. Phys. **59**, 87 (1978); Nucl. Phys. **A301**, 411 (1978); **A337**, 23 (1980). See also the earlier work of P. E. Shanley, Phys. Rev. **187**, 1328 (1969) and B. Charnomordic, C. Fayard, and G. H. Lamot, Phys. Rev. C **15**, 864 (1977).
- <sup>4</sup>J. Bang and C. Gignoux, Nucl. Phys. **A313**, 119 (1979).
- <sup>5</sup>Y. Matsui, Phys. Rev. C **22**, 2591 (1980).
- <sup>6</sup>M. Rai, D. R. Lehman, and A. Ghovanlou, Phys. Lett. **59B**, 327 (1975).
- <sup>7</sup>A preliminary account of this work can be found in D. R. Lehman, in Proceedings of the Ninth International Conference on the Few-Body Problem, Eugene, Oregon, 1980, Vol. I, p. 53.
- <sup>8</sup>D. Albrecht, M. Csatlós, J. Erö, Z. Fodor, I. Hernyes, Hongsung Mu, B. A. Khomenko, N. N. Khovanskij, P. Koncz, Z. V. Krumstein, Yu. P. Merkov, V. I. Petrukhin, Z. Seres, and L. Végh, Nucl. Phys. **A338**, 477 (1980).
- <sup>9</sup>V. V. Balashov, in *Clustering Aspects of Nuclear Structure and Nuclear Reactions, Winnipeg, 1978*, Proceedings of the Third International Conference on Clustering Aspects of Nuclear Structure and Nuclear Reactions, edited by W. T. H. van Oers, J. P. Svenne, J. S. C. McKee, and W. R. Falk (AIP, New York, 1978), p. 252.
- <sup>10</sup>L. Végh and J. Erö, Phys. Rev. C **23**, 2371 (1981).
- <sup>11</sup>J. V. Noble, Phys. Lett. **55B**, 433 (1975).
- <sup>12</sup>A. R. Edmonds, *Angular Momentum in Quantum Mechanics* (Princeton University, Princeton, 1957).
- <sup>13</sup>M. P. Bornand, G. R. Plattner, R. D. Viollier, and K. Alder, Nucl. Phys. **A294**, 492 (1978); G. R. Plattner, M. Bornand, and K. Alder, Phys. Lett. **61B**, 21 (1976).
- <sup>14</sup>D. Bachelier, Ph.D. thesis, Faculté des Sciences, Orsay, University of Paris, 1971 (unpublished).
- <sup>15</sup>P. Kitching, W. C. Olsen, H. S. Sherif, W. Dollhopf, C. Lunke, C. F. Perdrisat, J. R. Priest, and W. K. Roberts, Phys. Rev. C **11**, 420 (1975); W. Dollhopf, C. F. Perdrisat, P. Kitching, and W. C. Olsen, Phys. Lett. **58B**, 425 (1975).
- <sup>16</sup>P. G. Roos, N. S. Chant, A. A. Cowley, D. A. Goldberg, H. D. Holmgren, and R. Woody III, Phys. Rev. C **15**, 69 (1977).
- <sup>17</sup>A. A. Cowley, P. G. Roos, N. S. Chant, R. Woody III, H. D. Holmgren, and D. A. Goldberg, Phys. Rev. C **15**, 1650 (1977).
- <sup>18</sup>As can be seen from the second paper (LRG) of Ref. 1 above, where the  ${}^6\text{Li}$  ground-state binding energy (BE) is computed for several values of the percentage  $D$  state in the deuteron ( $P_D$ ), the binding energy is highly correlated linearly to the  $D$ -state percentage:  $\text{BE} = (-0.086 \pm 0.004)P_D + (4.44 \pm 0.02)$  in MeV. Also, in LRG, column six of Table VIII, the fifth entry should read  $-9.200(-2)$ .
- <sup>19</sup>S. Barbarino, M. Lattuada, F. Riggi, C. Spitaleri, and D. Vinciguerra, Phys. Rev. C **21**, 1104 (1980).
- <sup>20</sup>J. Erö, private communication.
- <sup>21</sup>N. S. Craigie and C. Wilkin, Nucl. Phys. **B14**, 477 (1969).
- <sup>22</sup>For a start in that direction, see L. Végh, J. Phys. G **5**, L121 (1979).
- <sup>23</sup>It is not clear whether distortion effects will fill in the minimum for a 600 MeV incident energy  ${}^6\text{Li}(p, p\alpha)d$  or  ${}^6\text{Li}(p, pd)\alpha$  experiment. Distortion does fill in the minimum when the incident energy is  $\leq 100$  MeV. See Ref. 16; also N. S. Chant and P. G. Roos, Phys. Rev. C **15**, 57 (1977). It would be valuable to perform DWIA compared to PWIA calculations for incident energies in the range 100 to 600 MeV for  ${}^6\text{Li}(p, p\alpha)d$  to

see if filling of the minimum persists.

<sup>24</sup>J. V. Noble, Phys. Rev. C 9, 1209 (1974).

<sup>25</sup>F. C. Barker, Nucl. Phys. 83, 418 (1966).

<sup>26</sup>S. Varma and P. Goldhammer, Nucl. Phys. A125, 193 (1969).

<sup>27</sup>These integrals are evaluated by the method of D. R. Lehman, W. C. Parke, and L. C. Maximon, J. Math. Phys. 22, 1399 (1981).

<sup>28</sup>E. L. Tomusiak generated the Woods-Saxon wave function.

<sup>29</sup> $C_0^{ad}$  is highly correlated linearly with the  ${}^6\text{Li}$  binding energy, but  $C_2^{ad}$  evidently does not have such a relationship. Specifically,  $C_0^{ad} = (0.351 \pm 0.009) \text{ BE} + (0.76 \pm 0.04)$ . Since BE is linearly related to  $P_D$  (see Ref. 18), we can estimate  $C_0^{ad} (P_D = 7\%) = 2.11 \pm 0.04$ .

<sup>30</sup>In this respect, we refer the reader to recent work on  ${}^3\text{He}$ . See J. L. Friar, B. F. Gibson, D. R. Lehman, and G. L. Payne, Phys. Rev. C 25, 1616 (1982). In this work, it is emphasized that asymptotic normalization constants be defined relative to zero-range comparison functions that are normalized to unity. That has not been done for the experimental values quoted in Table IV (see Ref. 13). If these values are adjusted so that they are defined relative to a normalized Whittaker function, we get  $1.86 \pm 0.05$  and  $0.01 \pm 0.03$  (rounded to proper significant figures), respectively. *Perhaps* these values (especially the  $S$  wave) compared to the full (4%) model give an indication of Coulomb effects, since the theoretical norms are defined relative to a normalized zero-range function [see Eqs. (5) and (8)].